

 Open access • Posted Content • DOI:10.1101/087585

Cobalt enrichment in anaerobic microbial cocultures revealed by synchrotron X-ray fluorescence imaging — [Source link](#)

Jennifer B. Glass, Si Chen, Katherine S. Dawson, Damian R Horton ...+4 more authors

Institutions: Georgia Institute of Technology, Argonne National Laboratory, California Institute of Technology, Bigelow Laboratory For Ocean Sciences

Published on: 14 Nov 2016 - bioRxiv (Cold Spring Harbor Laboratory)

Topics: Cobalt, Zinc and Copper

Related papers:

- [Trace Metal Imaging of Sulfate-Reducing Bacteria and Methanogenic Archaea at Single-Cell Resolution by Synchrotron X-Ray Fluorescence Imaging](#)
- [Electron microprobe and X-ray microfluorescence analyses of copper binding to active and inactivated cells of *Mucor rouxii*](#)
- [Sulfidogenic activity of sulfate and sulfur reducing bacteria under the influence of metal compounds](#)
- [Elemental composition of extremely alkaliphilic anaerobic bacteria](#)
- [Nickel sulfide, iron-nickel sulfide and iron sulfide precipitation by a newly isolated *Desulfotomaculum* species and its relation to nickel resistance](#)

Share this paper:    

View more about this paper here: <https://typeset.io/papers/cobalt-enrichment-in-anaerobic-microbial-cocultures-revealed-2l5ryz8vzr>

1 **Trace metal imaging of sulfate-reducing bacteria and methanogenic archaea**
2 **at single-cell resolution by synchrotron X-ray fluorescence imaging**

3 *Jennifer B. Glass*^{1*}, *Si Chen*², *Katherine S. Dawson*³, *Damian R. Horton*¹, *Stefan Vogt*², *Ellery D.*
4 *Ingall*¹, *Benjamin S. Twining*⁴, *Victoria J. Orphan*³

5 ¹School of Earth and Atmospheric Sciences, Georgia Institute of Technology, Atlanta, Georgia
6 USA;

7 ²Advanced Photon Source, Argonne National Laboratory, Argonne, Illinois, USA;

8 ³Division of Geological and Planetary Sciences, California Institute of Technology, Pasadena,
9 California, USA;

10 ⁴Bigelow Laboratory for Ocean Sciences, East Boothbay, Maine, 04544, USA;

11 **Keywords:** sulfate reduction, methanogen, metals, methanol, synchrotron x-ray fluorescence

12 **Running Head:** Single-cell X-ray imaging

13 ***Corresponding Author:** Jennifer.Glass@eas.gatech.edu

14

15 **Abstract**

16 Metal cofactors are required for many enzymes in anaerobic microbial respiration. This study
17 examined iron, cobalt, nickel, copper, and zinc in cellular and abiotic phases at the single-cell
18 scale for a sulfate-reducing bacterium (*Desulfococcus multivorans*) and a methanogenic archaeon
19 (*Methanosarcina acetivorans*) using synchrotron x-ray fluorescence microscopy. Relative
20 abundances of cellular metals were also measured by inductively coupled plasma mass
21 spectrometry. For both species, zinc and iron were consistently the most abundant cellular
22 metals. *M. acetivorans* contained higher nickel and cobalt content than *D. multivorans*, likely
23 due to elevated metal requirements for methylotrophic methanogenesis. Cocultures contained
24 spheroid zinc sulfides and cobalt/copper-sulfides.

25 **Introduction**

26 In anoxic natural and engineered environments, sulfate-reducing bacteria and methanogenic
27 archaea perform the last two steps of organic carbon respiration, releasing sulfide and methane.
28 Sulfate-reducing bacteria and methanogenic archaea can exhibit cooperative or competitive
29 interactions depending on sulfate and electron donor availability (Brileya et al. 2014; Bryant et
30 al. 1977; Ozuolmez et al. 2015; Stams and Plugge 2009). Methanol (CH₃OH), the simplest
31 alcohol, is an important substrate for industrial applications (Bertau et al. 2014) and microbial
32 metabolisms. In the presence of methanol, sulfate reduction and methanogenesis occur
33 simultaneously in cocultures (Dawson et al. 2015; Phelps et al. 1985), anoxic sediments (Finke et
34 al. 2007; Oremland and Polcin 1982), and anaerobic digesters (Spanjers et al. 2002; Weijma and
35 Stams 2001). Methanol has also been studied as a substrate for stimulating organochlorine
36 degradation in sediment reactors containing sulfate-reducing bacteria and methanogenic archaea
37 (Drzyzga et al. 2002).

38 Metalloenzymes are essential for both sulfate reduction and methylotrophic
39 methanogenesis (Barton et al. 2007; Ferry 2010; Glass and Orphan 2012; Thauer et al. 2010).
40 Iron is needed for cytochromes and iron-sulfur proteins in both types of organisms (Fauque and
41 Barton 2012; Pereira et al. 2011; Thauer et al. 2008). Cobalt and zinc are present in the first
42 enzymes in sulfate reduction (ATP sulfurylase, Sat; Gavel et al. 1998; Gavel et al. 2008), and
43 methylotrophic methanogenesis (methanol:coenzyme M methyltransferase; Hagemeyer et al.
44 2006). Nickel is found in the final enzyme in methanogenesis (methyl coenzyme M reductase;
45 Ermler et al. 1997), and zinc is present in the heterodisulfide reductase that recycles cofactors
46 for the methyl coenzyme M reductase enzyme (Hamann et al. 2007). Nickel and cobalt are
47 required by methanogenic archaea and sulfate-reducing bacteria that are capable of complete

48 organic carbon oxidization for carbon monoxide dehydrogenase/acetyl Co-A synthase in the
49 Wood-Ljungdahl CO₂ fixation pathway (Berg 2011; Ragsdale and Kumar 1996). Hydrogenases
50 containing Ni and Fe are functional in many, but not all, sulfate-reducing bacteria (Osburn et al.
51 2016; Pereira et al. 2011) and methylotrophic methanogens (Guss et al. 2009; Thauer et al.
52 2010). Evidence for high metabolic metal demands is provided by limited growth of
53 methanogenic archaea without Co and Ni supplementation in methanol-fed monocultures
54 (Scherer and Sahm 1981) and anaerobic bioreactors (Florencio et al. 1994; Gonzalez-Gil et al.
55 1999; Paulo et al. 2004; Zandvoort et al. 2003; Zandvoort et al. 2006).

56 Sulfate-reducing bacteria produce sulfide, which can remove toxic metals from
57 contaminated ecosystems due to precipitation of metal sulfides with low solubility (Paulo et al.
58 2015). Metal sulfides may also limit the availability of essential trace metals for microbial
59 metabolism (Glass and Orphan 2012; Glass et al. 2014). In sulfidic environments such as marine
60 sediments and anaerobic digesters, dissolved Co and Ni are present in nanomolar concentrations
61 (Glass et al. 2014; Jansen et al. 2005). These metals are predominantly present as solid metal
62 sulfide precipitates (Drzyzga et al. 2002; Luther III and Rickard 2005; Moreau et al. 2013)
63 and/or sorbed to anaerobic sludge (van Hullebusch et al. 2006; van Hullebusch et al. 2005; van
64 Hullebusch et al. 2004). The bioavailability of metals in these solid phases to anaerobic microbes
65 remains relatively unknown. Previous studies suggest that methanogenic archaea can leach Ni
66 from silicate minerals (Hausrath et al. 2007) and metal sulfides (Gonzalez-Gil et al. 1999; Jansen
67 et al. 2007). Sulfidic/methanogenic bioreactors (Jansen et al. 2005) and *D. multivorans*
68 monocultures (Bridge et al. 1999) contain high-affinity Co-/Ni- and Cu-/Zn-binding ligands,
69 respectively, which may aid in liberating metal micronutrients from solid phases when they
70 become growth-limiting.

71 Due to the importance of trace metals for anaerobic microbial metabolisms in
72 bioremediation and wastewater treatment, extensive efforts have focused on optimizing metal
73 concentrations to promote microbial organic degradation in anaerobic digesters (for review, see
74 Demirel and Scherer (2011)). Numerous studies have investigated the effect of heavy metals on
75 anaerobic metabolisms at millimolar concentrations in heavy-metal contaminated industrial
76 wastewaters, whereas few studies have investigated interactions between anaerobic microbes and
77 transition metals at the low micro- to nanomolar metal concentrations present in most natural
78 ecosystems and municipal wastewaters (see Paulo et al. 2015 for review). Studies of the metal
79 content of anaerobic microbes have primarily measured monocultures using non-spatially
80 resolved techniques such as ICP-MS (Barton et al. 2007; Cvetkovic et al. 2010; Scherer et al.
81 1983). Little is known about the effect of coculturing on cellular elemental composition and
82 mineralogy due to changes in geochemistry (e.g. via sulfide production) of the medium and/or
83 microbial metabolisms (e.g. via competition for growth-limiting substrates).

84 In this study, we measured cellular elemental contents and imaged extracellular metallic
85 minerals for sulfate-reducing bacteria and methanogenic archaea grown in mono- and co-culture.
86 For the model sulfate-reducing bacterium, we chose the metabolically versatile species
87 *Desulfococcus multivorans*, which is capable of complete organic carbon oxidation.
88 *Methanosarcina acetivorans* C2A, a well-studied strain capable of growing via acetivlastic and
89 methylotrophic methanogenesis, but not on H₂/CO₂, was selected as the model methanogenic
90 archaeon. These species were chosen because they are the most phylogenetically similar to pure
91 culture isolates available to syntrophic consortia of anaerobic methanotrophic euryarchaeota
92 (ANME-2) and sulfate-reducing bacteria (*Desulfosarcina/Desulfococcus*) partner that catalyze
93 the anaerobic oxidation of methane in marine sediments (see Dawson et al. (2015) for more on

94 coculture design). Individual cells of mono- and cocultures of these two species were imaged for
95 elemental content on the Bionanoprobe (Chen et al. 2013) at the Advanced Photon Source
96 (Argonne National Laboratory) and measured for relative abundance of bulk cellular metals by
97 ICP-MS.

98 **Materials and Methods**

99 *Culture growth conditions*

100 The growth medium contained (in g L⁻¹): NaCl, 23.4; MgSO₄·7H₂O, 9.44; NaHCO₃, 5.0; KCl,
101 0.8; NH₄Cl, 1.0; Na₂HPO₄, 0.6; CaCl₂·2H₂O, 0.14; cysteine-HCl, 0.25; resazurin, 0.001, 3 x 10⁻⁶
102 Na₂SeO₃ supplemented with DSM-141 vitamin (including 1 µg L⁻¹ vitamin B₁₂) and trace
103 element solutions containing metal concentrations (provided below as measured by ICP-MS) and
104 1.5 mg L⁻¹ nitrilotriacetic acid (Atlas 2010). The medium (pH 7.6) was filter sterilized in an
105 anoxic chamber (97% N₂ and 3% H₂ headspace) and reduced with 1 mM Na₂S.

106 Monocultures of *Desulfococcus multivorans* (DSM 2059) and *Methanosarcina*
107 *acetivorans* strain C2A (DSM 2834) were inoculated into 20 mL culture tubes containing 10 mL
108 of media with N₂:CO₂ (80:20) headspace, and sealed with butyl rubber stoppers and aluminum
109 crimp seals. *D. multivorans* monocultures were amended with filter-sterilized lactate (20 mM).
110 *M. acetivorans* monocultures were amended with filter-sterilized methanol (66 mM). Equal
111 proportions of dense monocultures in early stationary stage (as assessed by OD₆₀₀ measurements;
112 Fig. S1) were inoculated into sterile media and amended with filter-sterilized lactate (20 mM)
113 and methanol (66 mM) to form the coculture. Cultures were grown at 30°C without shaking.
114 After 12 days of growth (Fig. S1), mono- and cocultures were pelleted and frozen for ICP-MS
115 analysis, or prepared for SXRF imaging.

116 *Fluorescence in situ hybridization*

117 In order to confirm that monocultures were free of contamination, and to determine the relative
118 abundance of *D. multivorans* and *M. acetivorans* in coculture, fluorescence *in situ* hybridization
119 (FISH) was performed on separate aliquots from the same time point of the cell culture used for
120 SXRF analyses. One mL of cell culture was preserved in 3% paraformaldehyde for 1-3 hours,
121 then washed and resuspended in 200 μ L of 3x PBS:ethanol as described in Dawson et al. (2012).
122 Four microliters of fixed cells were spotted onto a glass slide and hybridized with an
123 oligonucleotide probe targeting *Methanosarcina acetivorans* MSMX860 (Raskin et al. 1994) and
124 the deltaproteobacterial probe Delta495a (Loy et al. 2002) and cDelta495a (Macalady et al.
125 2006). The FISH hybridization buffer contained 45% formamide, and the hybridization was
126 carried out at 46°C for 2 hours followed by a 15 minute wash in 48°C washing buffer (Daims et
127 al. 2005). The slides were rinsed briefly in distilled water, and mounted in a solution of DAPI (5
128 μ g/mL) in Citifluor AF-1 (Electron Microscopy Services). Imaging was performed with a 100x
129 oil immersion objective (Olympus PlanApo). Cell counts were performed by hand. Multiple
130 fields of view from replicate wells were compiled and counted on the basis of fluorescence in
131 DAPI (all cells), Cy3 (bacteria), and FITC (archaea).

132 ***ICP-MS***

133 Frozen cell pellets were dried (yielding ~4 mg dry weight per sample) in acid-washed Savillex
134 Teflon vials in a laminar flow hood connected to ductwork for exhausting acid fumes. Cells were
135 digested overnight at 150°C in 2 mL of trace metal grade nitric acid and 200 μ L hydrogen
136 peroxide, dried again, and dissolved in 5 mL 5% nitric acid. The medium was diluted 1:50 in
137 nitric acid. The elemental content of microbial cells and media was analyzed by ICP-MS
138 (Element-2, University of Maine Climate Change Institute). Sterile medium contained the

139 following concentrations (in μM): P, 800; Zn, 7; Fe, 4; Co, 2; Ni, 0.9; Cu, 0.3. Digestion acid
140 blanks contained (in nM): P, 127; Zn, 12; Fe, 5; Co, 0.007; Ni, 0.9; Mo, 0.02; Cu, 0.1; V, 0.03.

141 *SXRF sample preparation*

142 Monocultures were prepared for SXRF analysis without chemical fixation by spotting onto
143 silicon nitride (SiN) wafers (Silson Ltd., cat. 11107126) followed by rinsing with 10 mM HEPES
144 buffer (pH 7.8). To enable FISH microscopy after SXRF analysis, cocultures were chemically
145 preserved prior to analysis by incubation on ice for 1 hour in 50 mM HEPES and 0.6 M NaCl
146 (pH 7.2) containing 3.8% paraformaldehyde and 0.1% glutaraldehyde that had been cleaned of
147 potential trace-metal contaminants with cation exchange resin (Dowex 50-W X8) using
148 established protocols (Price et al. 1988; Twining et al. 2003). Cells were then centrifuged, re-
149 suspended in 10 mM HEPES buffer (pH 7.8) and either embedded in resin and thin sectioned
150 following the methods described in McGlynn et al. (2015) or spotted directly onto SiN wafers.

151 *SXRF analyses*

152 Whereas ICP-MS measurements cannot delineate the elemental contributions of co-occurring
153 cell types, SXRF imaging enables elemental quantification of the specific cell of interest (Fahrni
154 2007; Ingall et al. 2013; Kemner et al. 2004; Nuester et al. 2012; Twining et al. 2003; Twining et
155 al. 2008). SXRF analyses were performed at the Bionanoprobe (beamline 21-ID-D, Advanced
156 Photon Source, Argonne National Laboratory). Silicon nitride wafers were mounted
157 perpendicular to the beam as described in Chen et al. (2013). SXRF mapping was performed
158 with monochromatic 10 keV hard X-rays focused to a spot size of ~ 100 nm using Fresnel zone
159 plates. Concentrations and distributions of all elements from P to Zn were analyzed in fine scans
160 using a step size of 100 nm and a dwell time of 150 ms. An X-ray fluorescence thin film (AXO
161 DRESDEN, RF8-200-S2453) was measured with the same beamline setup as a reference. MAPS

162 software was used for per-pixel spectrum fitting and elemental content quantification (Vogt
163 2003). Sample elemental contents were computed by comparing fluorescence measurements
164 with a calibration curve derived from measurements of a reference thin film.

165 Regions of interest (ROIs) were selected with MAPS software by highlighting each
166 microbial cell (identified based on elevated P content with care taken to avoid regions of
167 elevated non-cellular metals) or particle (identified based on elevated metal content). Each ROI
168 (n=14 and n=17 for *D. multivorans* (radius: $0.60 \pm 0.01 \mu\text{m}$) and *M. acetivorans* (radius: $0.48 \pm$
169 $0.01 \mu\text{m}$), respectively, and n=13 for the coculture (radius: $0.96 \pm 0.01 \mu\text{m}$)) was background
170 corrected to remove elements originating from each section of the SiN grid on which cells were
171 spotted. To do so, the mean of triplicate measurements of area-normalized elemental content for
172 blank areas bordering the analyzed cells was subtracted from cellular ROIs. The background-
173 corrected area-normalized molar elemental content was then multiplied by cellular ROI area to
174 obtain molar elemental content per cell, which was then divided by the cell volume ($4/3\pi r^3$,
175 assuming spherical cells) to yield total metal content per cell volume, in units of mmol L^{-1} .
176 Visualization of elemental co-localization was performed with MAPS software. Statistical
177 analysis was performed with JMP Pro (v. 12.1.0) using the Tukey-Kramer HSD test.

178

179 **Results**

180 *Cellular elemental content of monocultures*

181 Cellular metal contents of *M. acetivorans* and *D. multivorans* monocultures followed the trend
182 $\text{Zn} \approx \text{Fe} > \text{Cu} > \text{Co} > \text{Ni}$ when measured by SXRF, and $\text{Zn} \approx \text{Fe} > \text{Co} > \text{Ni} > \text{Cu}$ when measured
183 by ICP-MS (Fig. 1). When normalized to cell volume, cellular S measured by SXRF was 50x
184 higher in methanol-grown *M. acetivorans* (n=14) than lactate-grown *D. multivorans* (n=17).

185 Cellular P, Fe, Co, Ni and Cu were 4-7x higher in *M. acetivorans* than *D. multivorans*, and
186 cellular Zn was not significantly different between the two microbes (Table 1).

187 ***Relative abundance of species in coculture***

188 Coculturing of both species for 12 days in media containing methanol and lactate resulted in
189 dominance of *M. acetivorans* (77%, or 1,753 cells hybridized with the MSMX860 FISH probe)
190 over *D. multivorans* (23%, or 522 cells hybridized with the Delta495a FISH probe) for 2,275
191 total cells counted in ten 100x (125 x 125 μm) fields of view. Cells were $\sim 1 \mu\text{m}^2$ cocci. No other
192 cells exhibited DAPI staining other than those that hybridized with MSMX860 and Delta495a
193 oligonucleotide probes. Attempts at FISH microscopy after SXRF analysis were unsuccessful
194 due to x-ray radiation damage of the cells.

195 ***Cellular elemental content of cocultures***

196 ICP-MS measurements showed that the relative abundance of cellular metals remained relatively
197 constant between mono- and cocultures, whereas SXRF data indicated that the coculture
198 contained a relatively higher proportion of Co than the monocultures (Fig. 1). SXRF imaging
199 showed no visual difference in elemental distribution between cells in the coculture (Fig. 2),
200 although the relatively small size of the cells relative to the focused x-ray spot may have limited
201 our ability to discern subtle differences. Cocultures, which were fixed with paraformaldehyde
202 and glutaraldehyde for subsequent fluorescence microscopy, were larger (radius: 0.96 ± 0.01
203 μm) than monocultures (*D. multivorans* radius: $0.60 \pm 0.01 \mu\text{m}$; *M. acetivorans* radius: $0.48 \pm$
204 $0.01 \mu\text{m}$), which were not fixed prior to analysis. When normalized on a per cell basis,
205 cocultures contained 5-20x higher P, Co and Ni than monocultures; however, when normalized
206 to cellular volume, the larger cell volumes of the cocultures resulted in significantly less Fe, Cu
207 and Zn per cellular volume than either of the monocultures (Table 1).

208 *Non-cellular metals in cocultures*

209 In whole cell SXRF images, ~30 “hot spots” (discrete semi-circular areas with low-P and
210 elevated metals, indicative of nano-sized minerals) of Zn (max: $0.7 \mu\text{g cm}^{-2}$), Co (max: $0.4 \mu\text{g}$
211 cm^{-2}) and S (max: $2.7 \mu\text{g cm}^{-2}$) were present in the center of a cluster of ~30 cocultured cells
212 identified as P-containing cocci (Fig. 2). In thin sections, semi-circular non-cellular small Zn hot
213 spots ($0.6 \pm 0.1 \mu\text{m}^2$) containing ~1:1 molar ratios of Zn:S ($17 \pm 2 \mu\text{g Zn cm}^{-2}$: $7.6 \pm 0.7 \mu\text{g S}$
214 cm^{-2}) were interspersed amongst cell clusters (n=8; Fig. 3a-e) along with more numerous
215 spheroid non-cellular Co hot spots of the same size ($0.6 \pm 0.1 \mu\text{m}^2$) containing $2.1 \pm 0.1 \mu\text{g Co}$
216 cm^{-2} , $3.4 \pm 0.2 \mu\text{g S cm}^{-2}$, and $1.3 \pm 0.1 \mu\text{g Cu cm}^{-2}$ (n=45; Fig. 3a-e). Discrete semi-circular hot
217 spots of elevated Ni (max: $2.9 \mu\text{g cm}^{-2}$) with low S were observed in two imaging fields (n=8;
218 Fig. 3b,c).

219

220 **Discussion**

221 In this study, SXRF imaging and quantification of trace metals in cellular and abiotic phases was
222 performed at the single-cell scale. Our observation that Zn and Fe were the two most abundant
223 cellular trace metals in monocultures is consistent with previous studies of diverse prokaryotes
224 (Barton et al. 2007; Cvetkovic et al. 2010; Outten and O'Halloran 2001; Rouf 1964), including
225 diverse mesophilic and hyperthermophilic methanogens grown on a range of substrates, for
226 which, generally: Fe > Zn > Ni > Co > Cu (Cameron et al. 2012; Scherer et al. 1983). To our
227 knowledge, there are no previous reports of the trace metal content of sulfate-reducing bacteria,
228 but the abundance of Fe and Zn-containing proteins encoded by their genomes (Barton and
229 Fauque 2009; Barton et al. 2007; Fauque and Barton 2012) is consistent with the cellular
230 enrichment we observed in these trace metals.

231 Both normalizations for SXRF data (per cell and per cellular volume) showed that the
232 methanogenic archaeon contained more P, S, Co, Ni and Cu than the sulfate-reducing bacterium.
233 The higher cellular Co content of *M. acetivorans* vs. *D. multivorans* is likely due to due to
234 numerous methyltransferases involved in methylotrophic methanogenesis (Zhang and Gladyshev
235 2010; Zhang et al. 2009) that contain cobalt as a metal center in their corrinoid (vitamin B₁₂)
236 cofactor, in addition to the corrinoid-containing Fe-S methyltransferase protein in the Wood
237 Ljungdahl pathway in both species (Ekstrom and Morel 2008; Fig. 4). Similarly, the higher Ni
238 content of *M. acetivorans* vs. *D. multivorans* is likely due to the presence of Ni-containing
239 cofactor F₄₃₀ in methyl coenzyme M reductase, the final enzyme in the methanogenesis pathway.
240 Cofactor F₄₃₀ is found only in methane-metabolizing archaea, in which it comprises 50-80% of
241 total cellular Ni (Diekert et al. 1981; Mayr et al. 2008). Additional Ni requirements in both *M.*
242 *acetivorans* and *D. multivorans* are used for Ni-Fe hydrogenases and carbon monoxide
243 dehydrogenase in the Wood-Ljungdahl pathway (Fig. 4).

244 Metabolic Cu requirements for methanogenesis are not well known, although high
245 accumulations have also been reported for other methanogens (Scherer et al. 1983). However, it
246 should be noted that our early trials analyzing S-rich cells on Au grids revealed artifacts resulting
247 from interactions of S and Cu underlying the grid's surface Au coating (data not shown); use of
248 SiN grids in this study appeared to eliminate such Cu artifacts, but potential reactions between
249 trace Cu in SiN grids and abundant S in the archaeal cells cannot be completely discounted.

250 Faster growth rates of methylotrophic methanogens than sulfate-reducing bacteria at
251 moderate temperatures have been reported in previous studies (Dawson et al. 2015; Weijma and
252 Stams 2001), and likely account for *M. acetivorans* outcompeting *D. multivorans* in our
253 cocultures. We consider it unlikely that differences in cellular trace metal contents in

254 monocultures were a result of harvesting *D. multivorans* earlier in their stationary phase than *M.*
255 *acetivorans* (Fig. S1) because cellular metal reserves generally decline or remain constant in
256 stationary phase (Bellenger et al. 2011). Our SXRF measurements of cocultures are more
257 difficult to interpret due to apparent swelling of aldehyde-fixed cocultured cells (~1 μm radius)
258 to ~2x the size of monocultures (0.5-0.6 μm radius). When normalized per cell, fixed cocultures
259 showed significantly higher P, Co and Ni than unfixed monocultures, but the apparent swelling
260 of cocultured cells erased this trend when normalized to cellular volume.

261 When grown at millimolar metal concentrations, sulfate-reducing bacteria efficiently
262 remove metals from solution (Krumholz et al. 2003) and precipitate covellite (CuS; Gramp et al.
263 2006; Karnachuk et al. 2008), sphalerite/wurtzite (ZnS/(Zn,Fe)S; Gramp et al. 2007; Xu et al.
264 2016), and pentlandite (Co₉S₈) (Sitte et al. 2013). Based on its ~1:1 Zn:S ratio, the semi-circular
265 nanoparticulate zinc sulfide phase(s) observed in thin sections imaged by SXRF in this study
266 were likely sphalerite spheroids, also found in sulfate-reducing bacteria biofilms due to
267 aggregation of ZnS nanocrystals (0.1-10 μm) and extracellular proteins (Moreau et al. 2004;
268 Moreau et al. 2007). The abiotic phase with the approximate stoichiometry (CoCu)S₂ may be
269 mineralogically distinct from those in previous studies.

270

271 **Conclusions and Challenges**

272 This study used two independent methods for assessing trace metal inventories in anaerobic
273 microbial cultures. We found that SXRF is a promising method for imaging and quantifying
274 first-row transition metals in anaerobic microbial cultures at single-cell resolution. This method's
275 single-cell resolution enables more precise measurements of cellular metal content than ICP-MS
276 analysis of bulk cells, which can include metals bound to extracellular aggregations such as

277 cation-binding exopolymeric substances produced by sulfate-reducing bacteria (Beech and
278 Cheung 1995; Beech et al. 1999; Braissant et al. 2007). We did not observe evidence of metal
279 contamination from aldehyde fixation in SXRF data, likely because we pre-cleaned fixatives
280 with metal-chelating resin prior to use, as previously described by Twining et al. (2003).

281 Challenges remain with accurate elemental quantification of microbial cocultures
282 preserved in a manner that would also allow assignment of identity for similar cell types. It was
283 not possible to distinguish methanogenic archaea from sulfate-reducing bacteria in coculture on
284 the basis of cell morphology or elemental content, and attempts to image cells with fluorescent
285 oligonucleotide probes after SXRF analysis were unsuccessful due to x-ray radiation damage.
286 We recommend method development for simultaneous taxonomic identification and elemental
287 imaging (e.g. gold-FISH (Schmidt et al. 2012)) for samples containing multiple microbial
288 species as a high priority for future work.

289 **Author Contributions**

290 J.B.G., V.J.O., S.C., and K.S.D. conceived and designed the experiments; K.S.D. performed the
291 microbial culturing, S.C., J.B.G., and S.V. performed the SXRF analyses; B.S.T. performed the
292 ICP-MS analysis, J.B.G., S.C., D.R.H., S.V., E.D.I., and B.S.T. analyzed the data; and J.B.G.
293 wrote the manuscript with input from all authors. All authors have given approval to the final
294 version of the manuscript.

295 **Funding Sources**

296 This work was supported by a NASA Astrobiology Postdoctoral Fellowship to J.B.G, NASA
297 Exobiology award NNX14AJ87G to J.B.G., DOE Biological and Environmental Research award
298 DE-SC0004949 to V.J.O, and NSF award OCE-0939564 to V.J.O. Use of the Advanced Photon
299 Source, an Office of Science User Facility operated for the U.S. DOE Office of Science by
300 Argonne National Laboratory, was supported by the U.S. DOE under Contract No. DE-AC02-
301 06CH11357. Use of the LS-CAT Sector 21 was supported by the Michigan Economic
302 Development Corporation and the Michigan Technology Tri-Corridor (Grant 085P1000817). We
303 thank two anonymous reviewers for helpful feedback on the previous version of this manuscript.

304 **Acknowledgements**

305 We thank Shawn McGlynn for assistance with sample preparation, and Keith Brister, Junjing
306 Deng, Barry Lai and Rachel Mak at LS-CAT for assistance with Bionanoprobe analysis. We
307 thank Larry Barton and Joel Kostka for helpful discussions, and Marcus Bray, Amanda Cavazos,
308 Grayson Chadwick, Chloe Stanton, and Nadia Szeinbaum for feedback on previous manuscript
309 drafts.

310

311 **Table 1.** Mean and standard error (in parentheses) of elemental contents normalized per cellular
 312 volume and per cell as measured by SXRF. Monocultures were prepared without chemical
 313 fixation, and cocultures were prepared with paraformaldehyde and glutaraldehyde fixation,
 314 followed by spotting onto silicon nitride wafers as described in the text. A, B and C superscripts
 315 indicate statistically different elemental contents ($p < 0.05$ based on Tukey-Kramer HSD test).

Culture	Substrate (mM)	P	S	Fe	Co	Ni	Cu	Zn
		Element per cellular volume (mmol L ⁻¹)						
100% <i>Methanosarcina acetivorans</i> DSM 2834 (n = 14)	Methanol (66 mM)	382 ^A (47)	4553 ^A (458)	38 ^A (4)	3.1 ^A (0.3)	0.44 ^A (0.04)	11 ^A (1)	38 ^A (3)
100% <i>Desulfococcus multivorans</i> DSM 2059 (n = 17)	Lactate (20 mM)	55 ^B (7)	96 ^B (11)	22 ^B (4)	0.5 ^B (0.1)	0.11 ^B (0.02)	3 ^B (1)	36 ^A (10)
77% <i>Methanosarcina acetivorans</i> DSM 2834, 23% <i>Desulfococcus multivorans</i> DSM 2059 (n = 13)	Methanol (66 mM), lactate (20 mM)	353 ^A (32)	234 ^B (19)	3.6 ^C (0.3)	2.0 ^C (0.2)	0.15 ^B (0.01)	0.13 ^C (0.04)	2.4 ^B (0.2)
		Element per cell (mol x 10 ⁻¹⁸ cell ⁻¹)						
100% <i>Methanosarcina acetivorans</i> DSM 2834 (n = 14)	Methanol (66 mM)	178 ^A (28)	2167 ^A (318)	19 ^A (4)	1.5 ^A (0.2)	0.20 ^A (0.03)	5 ^A (1)	17 ^{AB} (2)
100% <i>Desulfococcus multivorans</i> DSM 2059 (n = 17)	Lactate (20 mM)	60 ^A (11)	107 ^B (19)	24 ^A (6)	0.5 ^A (0.1)	0.12 ^A (0.02)	3 ^A (1)	39 ^A (12)
77% <i>Methanosarcina acetivorans</i> DSM 2834, 23% <i>Desulfococcus multivorans</i> DSM 2059 (n = 13)	Methanol (66 mM), lactate (20 mM)	1252 ^B (69)	855 ^C (69)	13 ^A (1)	7 ^B (1)	2 ^B (1)	0.5 ^B (0.2)	9 ^B (1)

316

317 **Figure Captions**

318 **Figure 1.** Proportions of each cellular metal (Fe, Co, Ni, Cu and Zn) for monocultures of
319 *Methanosarcina acetivorans* (n=14), monocultures of *Desulfococcus multivorans* (n=18), and
320 cocultures of 77% *M. acetivorans* and 23% *D. multivorans* (n=12) measured by ICP-MS (bulk
321 measurement) and SXRF (single cell average).

322 **Figure 2.** SXRF co-localization of P (red), Co (green), and Zn (blue; left panel), and S (red), Ni
323 (green), and Cu (blue; right panel) for whole cells of 77% *Methanosarcina acetivorans* and 23%
324 *Desulfococcus multivorans* in coculture. Values in parentheses are maxima in $\mu\text{g cm}^{-2}$ for each
325 element.

326 **Figure 3.** SXRF co-localization of P (red), Co (green), and Zn (blue) in left panels, and S (red),
327 Ni (green), and Cu (blue) in right panels for five imaged fields of 5 μm thin sections of 77%
328 *Methanosarcina acetivorans* and 23% *Desulfococcus multivorans* cocultures. Values in
329 parentheses are maxima in $\mu\text{g cm}^{-2}$ for each element.

330 **Figure 4.** Schematic of metalloenzyme-containing metabolic pathways in the complete carbon-
331 oxidizing sulfate-reducing bacterium *Desulfococcus multivorans* and the methylotrophic
332 methanogenic archaeon *Methanosarcina acetivorans* as confirmed by genomic analyses. Nickel
333 (Acs, Cdh, Mcr) and cobalt (CFeSP, Mts, Mtr, and Sat) containing enzymes are labeled in bold.
334 Enzyme abbreviations: Acs/CFeSP: acetyl-CoA synthase/corrinoid-FeS protein; Cdh: carbon
335 monoxide dehydrogenase; Mts: methanol:coenzyme M methyltransferase; Mcr: methyl
336 coenzyme M reductase; Mtr: methyl-tetrahydromethanopterin:coenzyme M methyltransferase;
337 Sat: ATP sulfurylase.

338 **Figure S1.** Growth curves based on OD600 for the three cultures described in this study:
339 *Methanosarcina acetivorans* (white), *Desulfococcus multivorans* (light grey), and 77%
340 *Methanosarcina acetivorans* and 23% *Desulfococcus multivorans* cocultures (dark grey).
341

342 References

- 343 Atlas RM. 2010. Handbook of Microbiological Media. CRC press.
- 344 Barton LL, Fauque GD. 2009. Biochemistry, physiology and biotechnology of sulfate-reducing
345 bacteria. *Adv Appl Microbiol* 68:41-98.
- 346 Barton LL, Goulhen F, Bruschi M, Woodards NA, Plunkett RM, Rietmeijer FJM. 2007. The
347 bacterial metallome: composition and stability with specific reference to the anaerobic
348 bacterium *Desulfovibrio desulfuricans*. *Biometals* 20:291–302.
- 349 Beech I, Cheung CS. 1995. Interactions of exopolymers produced by sulphate-reducing bacteria
350 with metal ions. *Int Biodeter Biodegr* 35(1):59-72.
- 351 Beech I, Zinkevich V, Tapper R, Gubner R, Avci R. 1999. Study of the interaction of sulphate-
352 reducing bacteria exopolymers with iron using X-ray photoelectron spectroscopy and
353 time-of-flight secondary ionisation mass spectrometry. *J Microbiol Met* 36(1):3-10.
- 354 Bellenger JP, Wichard T, Xu Y, Kraepiel AML. 2011. Essential metals for nitrogen fixation in a
355 free living N₂ fixing bacterium: chelation, homeostasis and high use efficiency. *Environ*
356 *Microbiol* 13(6):1395–1411.
- 357 Berg IA. 2011. Ecological aspects of the distribution of different autotrophic CO₂ fixation
358 pathways. *Appl Environ Microbiol* 77(6):1925-1936.
- 359 Bertau M, Offermanns H, Plass L, Schmidt F, Wernicke H-J. 2014. Methanol: the basic chemical
360 and energy feedstock of the future. Springer.
- 361 Braissant O, Decho AW, Dupraz C, Glunk C, Przekop KM, Visscher PT. 2007. Exopolymeric
362 substances of sulfate-reducing bacteria: interactions with calcium at alkaline pH and
363 implication for formation of carbonate minerals. *Geobiology* 5(4):401-411.
- 364 Bridge TA, White C, Gadd GM. 1999. Extracellular metal-binding activity of the sulphate-
365 reducing bacterium *Desulfococcus multivorans*. *Microbiology* 145(10):2987-2995.
- 366 Brileya KA, Camilleri LB, Zane GM, Wall JD, Fields MW. 2014. Biofilm growth mode
367 promotes maximum carrying capacity and community stability during product inhibition
368 syntrophy. *Front Microbiol* 5:693.
- 369 Bryant M, Campbell LL, Reddy C, Crabill M. 1977. Growth of *Desulfovibrio* in lactate or
370 ethanol media low in sulfate in association with H₂-utilizing methanogenic bacteria. *Appl*
371 *Environ Microbiol* 33(5):1162-1169.
- 372 Cameron V, House CH, Brantley SL. 2012. A first analysis of metallome biosignatures of
373 hyperthermophilic archaea. *Archaea* 2012:12.
- 374 Chen S, Deng J, Yuan Y, Flachenecker C, Mak R, Hornberger B, Jin Q, Shu D, Lai B, Maser J,
375 Roehrig C, Paunesku T, Gleber SC, Vine DJ, Finney L, VonOsinski J, Bolbat M, Spink I,
376 Chen Z, Steele J, Trapp D, Irwin J, Feser M, Snyder E, Brister K, Jacobsen C, Woloschak
377 G, Vogt S. 2013. The Bionanoprobe: hard X-ray fluorescence nanoprobe with cryogenic
378 capabilities. *J Synchrotron Radiat* 21(1):66-75.
- 379 Cvetkovic A, Menon AL, Thorgersen MP, Scott JW, Poole II FL, Jenney Jr FE, Lancaster WA,
380 Praissman JL, Shanmukh S, Vaccaro BJ, Trauger SA, Kalisiak E, Apon JV, Siuzdak G,
381 Yannone SM, Tainer JA, Adams MWW. 2010. Microbial metalloproteomes are largely
382 uncharacterized. *Nature* 466:779-782.
- 383 Daims H, Stoecker K, Wagner M. 2005. Fluorescence in situ hybridization for the detection of
384 prokaryotes. In: Osborn AM, Smith CJ, editors. *Molecular Microbial Ecology*. Abingdon,
385 UK: Bios-Garland. p. 239.

- 386 Dawson K, Osburn M, Sessions A, Orphan V. 2015. Metabolic associations with archaea drive
387 shifts in hydrogen isotope fractionation in sulfate-reducing bacterial lipids in cocultures
388 and methane seeps. *Geobiology* 13(5):462-477.
- 389 Dawson KS, Strapoč D, Huizinga B, Lidstrom U, Ashby M, Macalady JL. 2012. Quantitative
390 fluorescence in situ hybridization analysis of microbial consortia from a biogenic gas
391 field in Alaska's Cook Inlet Basin. *Appl Environ Microbiol* 78(10):3599-3605.
- 392 Demirel B, Scherer P. 2011. Trace element requirements of agricultural biogas digesters during
393 biological conversion of renewable biomass to methane. *Biomass Bioenerg.* 35:992-998.
- 394 Diekert G, Konheiser U, Piechulla K, Thauer RK. 1981. Nickel requirement and factor F430
395 content of methanogenic bacteria. *J. Bacteriol.* 148(2):459-464.
- 396 Drzyzga O, El Mamouni R, Agathos SN, Gottschal JC. 2002. Dehalogenation of chlorinated
397 ethenes and immobilization of nickel in anaerobic sediment columns under sulfidogenic
398 conditions. *Envir Sci Tech* 36(12):2630-2635.
- 399 Ekstrom EB, Morel FMM. 2008. Cobalt limitation of growth and mercury methylation in sulfate-
400 reducing bacteria. *Environ Sci Tech* 42(1):93-99.
- 401 Ermler U, Grabarse W, Shima S, Goubeaud M, Thauer RK. 1997. Crystal structure of methyl-
402 coenzyme M reductase: the key enzyme of biological methane formation. *Science*
403 278(5342):1457-1462.
- 404 Fahrni CJ. 2007. Biological applications of X-ray fluorescence microscopy: exploring the
405 subcellular topography and speciation of transition metals. *Curr Opin Chem Biol*
406 11(2):121-127.
- 407 Fauque GD, Barton LL. 2012. Hemoproteins in dissimilatory sulfate- and sulfur-reducing
408 prokaryotes. *Adv Microbiol Physiol* 60:1-90.
- 409 Ferry JG. 2010. How to make a living by exhaling methane. *Ann Rev Microbiol* 64:453-473.
- 410 Finke N, Hoehler TM, Jørgensen BB. 2007. Hydrogen 'leakage' during methanogenesis from
411 methanol and methylamine: implications for anaerobic carbon degradation pathways in
412 aquatic sediments. *Environ Microbiol* 9(4):1060-1071.
- 413 Florencio L, Field JA, Lettinga G. 1994. Importance of cobalt for individual trophic groups in an
414 anaerobic methanol-degrading consortium. *Appl Environ Microbiol* 60(1):227-234.
- 415 Gavel OY, Bursakov SA, Calvete JJ, George GN, Moura JJG, Moura I. 1998. ATP sulfurylases
416 from sulfate-reducing bacteria of the genus *Desulfovibrio*. A novel metalloprotein
417 containing cobalt and zinc. *Biochem* 37:16225-16232.
- 418 Gavel OY, Bursakov SA, Rocco GD, Trincao J, Pickering IJ, George GN, Calvete JJ, Shnyrov
419 VL, Brondino CD, Pereira AS. 2008. A new type of metal-binding site in cobalt-and
420 zinc-containing adenylate kinases isolated from sulfate-reducers *Desulfovibrio gigas* and
421 *Desulfovibrio desulfuricans* ATCC 27774. *J Inorganic Biochem* 102(5):1380-1395.
- 422 Glass JB, Orphan VJ. 2012. Trace metal requirements for microbial enzymes involved in the
423 production and consumption of methane and nitrous oxide. *Front Microbiol* 3:61.
- 424 Glass JB, Yu H, Steele JA, Dawson KS, Sun S, Chourey K, Pan C, Hettich RL, Orphan VJ.
425 2014. Geochemical, metagenomic and metaproteomic insights into trace metal utilization
426 by methane-oxidizing microbial consortia in sulphidic marine sediments. *Environ*
427 *Microbiol* 16(6):1592-1611.
- 428 Gonzalez-Gil G, Kleerebezem R, Lettinga G. 1999. Effects of nickel and cobalt on kinetics of
429 methanol conversion by methanogenic sludge as assessed by on-line CH₄ monitoring.
430 *Appl Environ Microbiol* 65(4):1789-1793.

- 431 Gramp JP, Bigham JM, Sasaki K, Tuovinen OH. 2007. Formation of Ni-and Zn-sulfides in
432 cultures of sulfate-reducing bacteria. *Geomicrobiol J* 24(7-8):609-614.
- 433 Gramp JP, Sasaki K, Bigham JM, Karnachuk OV, Tuovinen OH. 2006. Formation of covellite
434 (CuS) under biological sulfate-reducing conditions. *Geomicrobiol J* 23(8):613-619.
- 435 Guss AM, Kulkarni G, Metcalf WW. 2009. Differences in hydrogenase gene expression between
436 *Methanosarcina acetivorans* and *Methanosarcina barkeri*. *J Bacteriol* 191(8):2826-2833.
- 437 Hagemeyer CH, Kruer M, Thauer RK, Warkentin E, Ermler U. 2006. Insight into the mechanism
438 of biological methanol activation based on the crystal structure of the methanol-
439 cobalamin methyltransferase complex. *Proc Natl Acad Sci* 103(50):18917–18922.
- 440 Hamann N, Mander GJ, Shokes JE, Scott RA, Bennati M, Hedderich R. 2007. A cysteine-rich
441 CCG domain contains a novel [4Fe-4S] cluster binding motif as deduced from studies
442 with subunit B of heterodisulfide reductase from *Methanothermobacter marburgensis*.
443 *Biochemistry* 46(44):12875-12885.
- 444 Hausrath EM, Liermann LJ, House CH, Ferry JG, Brantley SL. 2007. The effect of methanogen
445 growth on mineral substrates: will Ni markers of methanogen based communities be
446 detectable in the rock record? *Geobiology* 5(1):49-61.
- 447 Ingall ED, Diaz JM, Longo AF, Oakes M, Finney L, Vogt S, Lai B, Yager PL, Twining BS,
448 Brandes JA. 2013. Role of biogenic silica in the removal of iron from the Antarctic seas.
449 *Nature Comm* 4:1981.
- 450 Jansen S, Gonzalez-Gil G, van Leeuwen HP. 2007. The impact of Co and Ni speciation on
451 methanogenesis in sulfidic media—Biouptake versus metal dissolution. *Enzyme Microb*
452 *Tech* 40:823-830.
- 453 Jansen S, Steffen F, Threels WF, Van Leeuwen HP. 2005. Speciation of Co (II) and Ni (II) in
454 anaerobic bioreactors measured by competitive ligand exchange-adsorptive stripping
455 voltammetry. *Environ Sci Tech* 39(24):9493-9499.
- 456 Karnachuk OV, Sasaki K, Gerasimchuk AL, Sukhanova O, Ivashenko DA, Kaksonen AH,
457 Puhakka JA, Tuovinen OH. 2008. Precipitation of Cu-sulfides by copper-tolerant
458 *Desulfovibrio* isolates. *Geomicrobiol J* 25(5):219-227.
- 459 Kemner KM, Kelly SD, Lai B, Maser J, O'loughlin EJ, Sholto-Douglas D, Cai Z, Schneegurt
460 MA, Kulpa CF, Nealson KH. 2004. Elemental and redox analysis of single bacterial cells
461 by X-ray microbeam analysis. *Science* 306(5696):686-687.
- 462 Krumholz LR, Elias DA, Suflita JM. 2003. Immobilization of cobalt by sulfate-reducing bacteria
463 in subsurface sediments. *Geomicrobiol J* 20(1):61-72.
- 464 Loy A, Lehner A, Lee N, Adamczyk J, Meier H, Ernst J, Schleifer K-H, Wagner M. 2002.
465 Oligonucleotide microarray for 16S rRNA gene-based detection of all recognized
466 lineages of sulfate-reducing prokaryotes in the environment. *Appl Environ Microbiol*
467 68(10):5064-5081.
- 468 Luther III GW, Rickard DT. 2005. Metal sulfide cluster complexes and their biogeochemical
469 importance in the environment. *J Nanopart Res* 7(4-5):389-407.
- 470 Macalady JL, Lyon EH, Koffman B, Albertson LK, Meyer K, Galdenzi S, Mariani S. 2006.
471 Dominant microbial populations in limestone-corroding stream biofilms, Frasassi cave
472 system, Italy. *Appl Environ Microbiol* 72(8):5596-5609.
- 473 Mayr S, Latkoczy C, Kruger M, Gunther D, Shima S, Thauer RK, Widdel F, Jaun B. 2008.
474 Structure of an F430 variant from archaea associated with anaerobic oxidation of
475 methane. *J Am Chem Soc* 130(32):10758-10767.

- 476 McGlynn SE, Chadwick GL, Kempes CP, Orphan VJ. 2015. Single cell activity reveals direct
477 electron transfer in methanotrophic consortia. *Nature* 526:531–535.
- 478 Moreau JW, Fournelle JH, Banfield JF. 2013. Quantifying heavy metals sequestration by sulfate-
479 reducing bacteria in an acid mine drainage-contaminated natural wetland. *Front*
480 *Microbiol* 4:43.
- 481 Moreau JW, Webb RI, Banfield JF. 2004. Ultrastructure, aggregation-state, and crystal growth of
482 biogenic nanocrystalline sphalerite and wurtzite. *Am Mineral* 89(7):950-960.
- 483 Moreau JW, Weber PK, Martin MC, Gilbert B, Hutcheon ID, Banfield JF. 2007. Extracellular
484 proteins limit the dispersal of biogenic nanoparticles. *Science* 316(5831):1600-1603.
- 485 Nuester J, Vogt S, Newville M, Kustka AB, Twining BS. 2012. The unique biochemical
486 signature of the marine diazotroph *Trichodesmium*. *Front Microbiol* 3:1-15.
- 487 Oremland RS, Polcin S. 1982. Methanogenesis and sulfate reduction: competitive and
488 noncompetitive substrates in estuarine sediments. *Appl Environ Microbiol* 44(6):1270-
489 1276.
- 490 Osburn MR, Dawson KS, Fogel ML, Sessions AL. 2016. Fractionation of hydrogen isotopes by
491 sulfate-and nitrate-reducing bacteria. *Front Microbiol* 7.
- 492 Outten CE, O'Halloran TV. 2001. Femtomolar sensitivity of metalloregulatory proteins
493 controlling zinc homeostasis. *Science* 292(5526):2488-2492.
- 494 Ozuolmez D, Na H, Lever MA, Kjeldsen KU, Jørgensen BB, Plugge CM. 2015. Methanogenic
495 archaea and sulfate reducing bacteria co-cultured on acetate: teamwork or coexistence?
496 *Front Microbiol* 6:492.
- 497 Paulo LM, Stams AJ, Sousa DZ. 2015. Methanogens, sulphate and heavy metals: a complex
498 system. *Rev Environ Sci Biotech* 14(4):537-553.
- 499 Paulo PL, Jiang B, Cysneiros D, Stams AJM, Lettinga G. 2004. Effect of cobalt on the anaerobic
500 thermophilic conversion of methanol. *Biotech Bioeng* 85(4):434-441.
- 501 Pereira IAC, Ramos AR, Grein F, Marques MC, Da Silva SM, Venceslau SS. 2011. A
502 comparative genomic analysis of energy metabolism in sulfate reducing bacteria and
503 archaea. *Front Microbiol* 2(69):1-22.
- 504 Phelps T, Conrad R, Zeikus J. 1985. Sulfate-dependent interspecies H₂ transfer between
505 *Methanosarcina barkeri* and *Desulfovibrio vulgaris* during coculture metabolism of
506 acetate or methanol. *Appl Environ Microbiol* 50(3):589-594.
- 507 Price NM, Harrison GI, Hering JG, Hudson RJ, Nirel PM, Palenik B, Morel FM. 1988.
508 Preparation and chemistry of the artificial algal culture medium Aquil. *Biol Oceanogr*
509 6(5-6):443-461.
- 510 Ragsdale SW, Kumar M. 1996. Nickel-containing carbon monoxide dehydrogenase/acetyl-CoA
511 synthase. *Chem Rev* 96(7):2515-2540.
- 512 Raskin L, Poulsen LK, Noguera DR, Rittmann BE, Stahl DA. 1994. Quantification of
513 methanogenic groups in anaerobic biological reactors by oligonucleotide probe
514 hybridization. *Appl Environ Microbiol* 60(4):1241-1248.
- 515 Rouf M. 1964. Spectrochemical analysis of inorganic elements in bacteria. *J Bacteriol*
516 88(6):1545-1549.
- 517 Scherer P, Lippert H, Wolff G. 1983. Composition of the major elements and trace elements of
518 10 methanogenic bacteria determined by inductively coupled plasma emission
519 spectrometry. *Biol Trace Elem Res* 5(3):149-163.
- 520 Scherer P, Sahn H. 1981. Effect of trace elements and vitamins on the growth of
521 *Methanosarcina barkeri*. *Acta Biotechnol* 1(1):57-65.

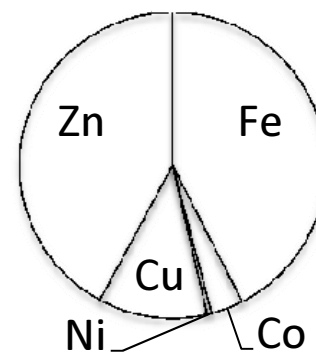
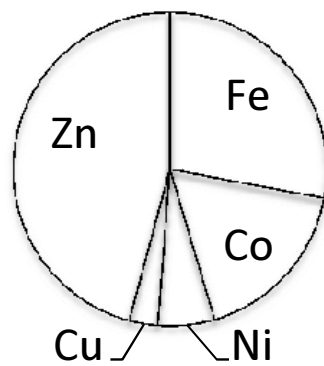
- 522 Schmidt H, Eickhorst T, Mußmann M. 2012. Gold-FISH: a new approach for the in situ
523 detection of single microbial cells combining fluorescence and scanning electron
524 microscopy. *System Appl Microbiol* 35(8):518-525.
- 525 Sitte J, Pollok K, Langenhorst F, Küsel K. 2013. Nanocrystalline nickel and cobalt sulfides
526 formed by a heavy metal-tolerant, sulfate-reducing enrichment culture. *Geomicrobiol J*
527 30(1):36-47.
- 528 Spanjers H, Weijma J, Abusam A. 2002. Modelling the competition between sulphate reducers
529 and methanogens in a thermophilic methanol-fed bioreactor. *Water Sci Tech* 45(10):93-
530 98.
- 531 Stams AJ, Plugge CM. 2009. Electron transfer in syntrophic communities of anaerobic bacteria
532 and archaea. *Nat Rev Microbiol* 7(8):568-577.
- 533 Thauer RK, Kaster A-K, Goenrich M, Schick M, Hiromoto T, Shima S. 2010. Hydrogenases
534 from methanogenic archaea, nickel, a novel cofactor, and H₂ storage. *Ann Rev Biochem*
535 79:507-536.
- 536 Thauer RK, Kaster A-K, Seedorf H, Buckel W, Hedderich R. 2008. Methanogenic archaea:
537 ecologically relevant differences in energy conservation. *Nat Rev Microbiol* 6:579-591.
- 538 Twining BS, Baines SB, Fisher NS, Maser J, Vogt S, Jacobsen C, Tovar-Sanchez A, Sanudo-
539 Wilhelmy SA. 2003. Quantifying trace elements in individual aquatic protist cells with a
540 synchrotron X-ray fluorescence microprobe. *Anal Chem* 75(15):3806-3816.
- 541 Twining BS, Baines SB, Vogt S, de Jonge MD. 2008. Exploring ocean biogeochemistry by
542 single-cell microprobe analysis of protist elemental composition. *J Eukaryot Microbiol*
543 55(3):151-162.
- 544 van Hullebusch ED, Gieteling J, Zhang M, Zandvoort MH, Daele WV, Defrancq J, Lens PNL.
545 2006. Cobalt sorption onto anaerobic granular sludge: Isotherm and spatial localization
546 analysis. *J Biotechnol* 121(2):227-240.
- 547 van Hullebusch ED, Peerbolte A, Zandvoort MH, Lens PNL. 2005. Sorption of cobalt and nickel
548 on anaerobic granular sludges: isotherms and sequential extraction. *Chemosphere*
549 58(4):493-505.
- 550 van Hullebusch ED, Zandvoort MH, Lens PNL. 2004. Nickel and cobalt sorption on anaerobic
551 granular sludges: kinetic and equilibrium studies. *J Chem Tech Biotech* 79(11):1219-
552 1227.
- 553 Vogt S. 2003. MAPS: A set of software tools for analysis and visualization of 3D X-ray
554 fluorescence data sets. *J Phys IV* 104:635-638.
- 555 Weijma J, Stams A. 2001. Methanol conversion in high-rate anaerobic reactors. *Water Sci Tech*
556 44(8):7-14.
- 557 Xu J, Murayama M, Roco CM, Veeramani H, Michel FM, Rimstidt JD, Winkler C, Hochella
558 MF. 2016. Highly-defective nanocrystals of ZnS formed via dissimilatory bacterial
559 sulfate reduction: A comparative study with their abiogenic analogues. *Geochem*
560 *Cosmochim Acta* 180:1-14.
- 561 Zandvoort MH, Geerts R, Lettinga G, Lens PNL. 2003. Methanol degradation in granular sludge
562 reactors at sub-optimal metal concentrations: role of iron, nickel and cobalt. *Enzyme*
563 *Microbiol Tech* 33(2-3):190-198.
- 564 Zandvoort MH, van Hullebusch ED, Gieteling J, Lens PNL. 2006. Granular sludge in full-scale
565 anaerobic bioreactors: trace element content and deficiencies. *Enzyme Microbiol Tech*
566 39(2):337-346.

- 567 Zhang Y, Gladyshev VN. 2010. dbTEU: a protein database of trace element utilization.
568 Bioinformatics 26(5):700-702.
- 569 Zhang Y, Rodionov DA, Gelfand MS, Gladyshev VN. 2009. Comparative genomic analyses of
570 nickel, cobalt and vitamin B12 utilization. BMC Genomics 10(78):1-26.
- 571

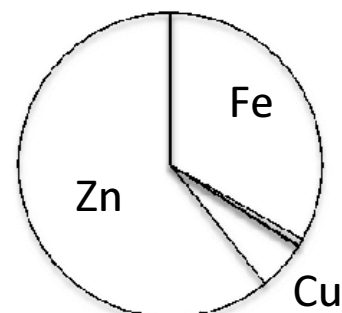
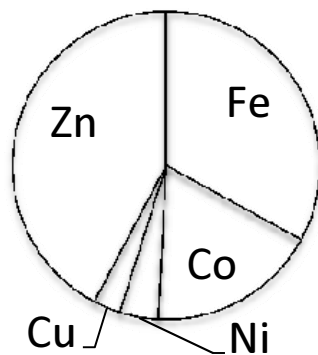
ICP-MS

SXRF

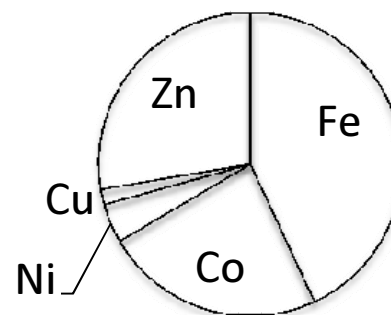
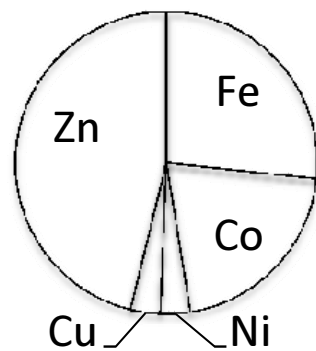
100%
Methanosarcina
acetivorans



100%
Desulfococcus
multivorans

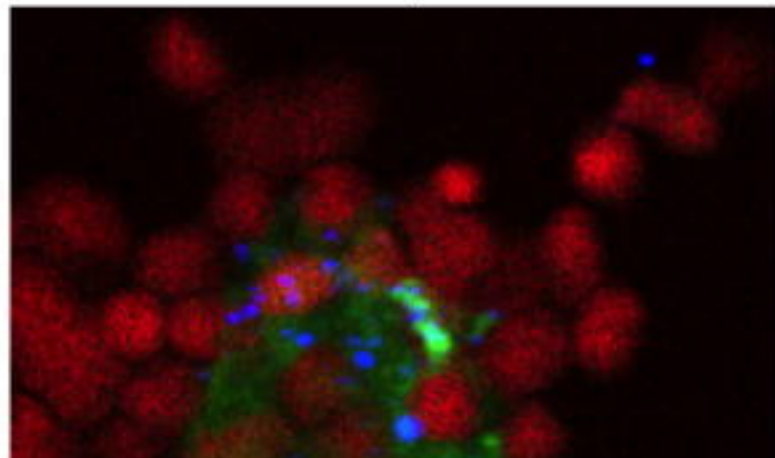


77% *Methanosarcina*
acetivorans,
23% *Desulfococcus*
multivorans

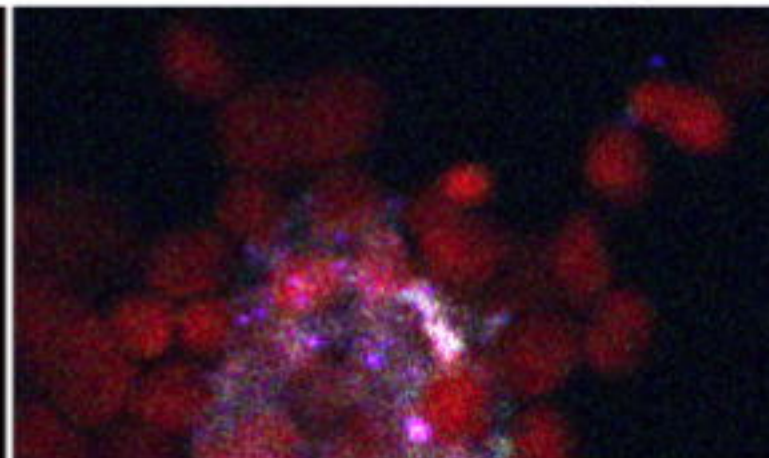


10 μm

Figure 2



P (3.5) Co (0.4) Zn (0.7)



S (2.7) Ni (0.03) Cu (0.04)

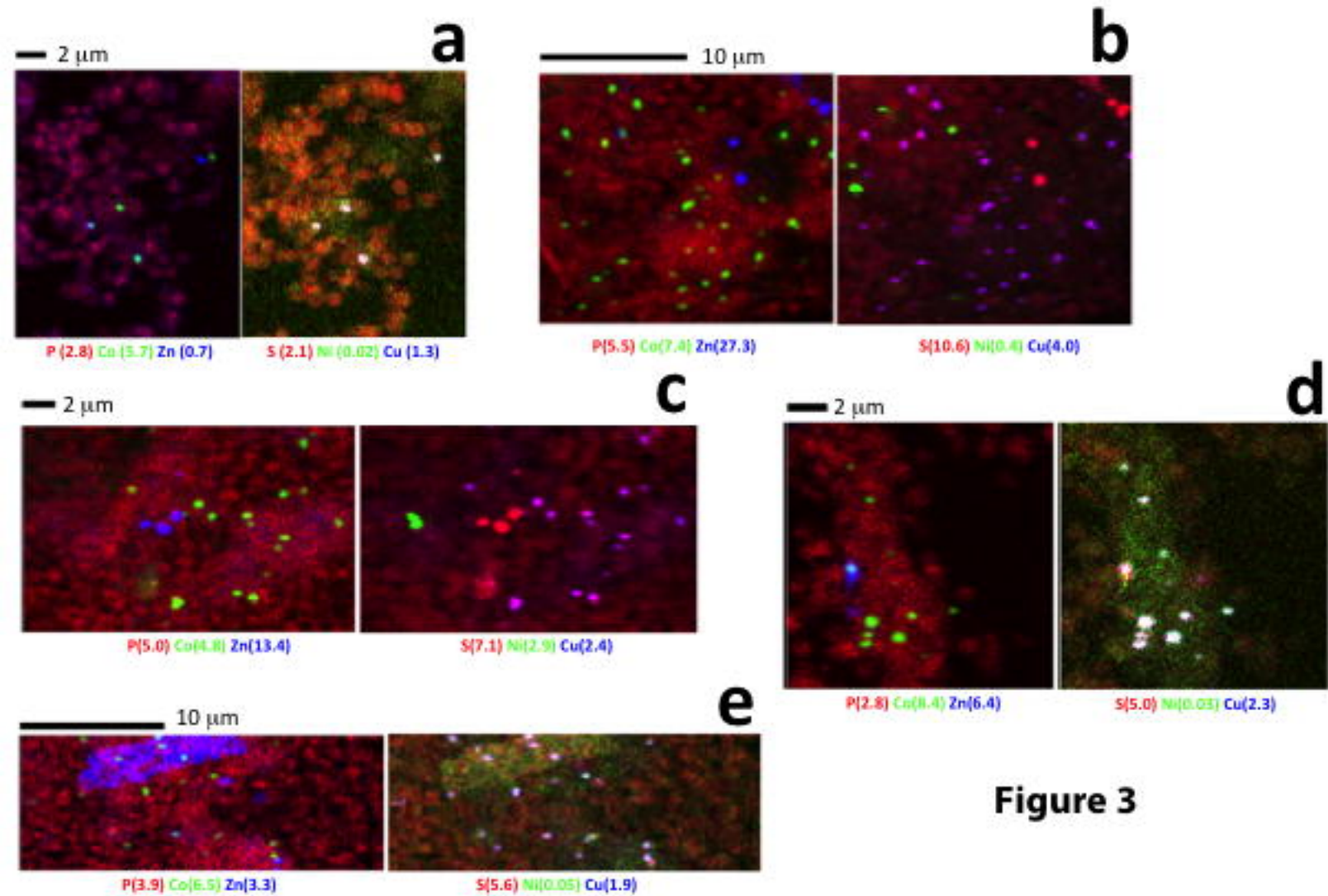
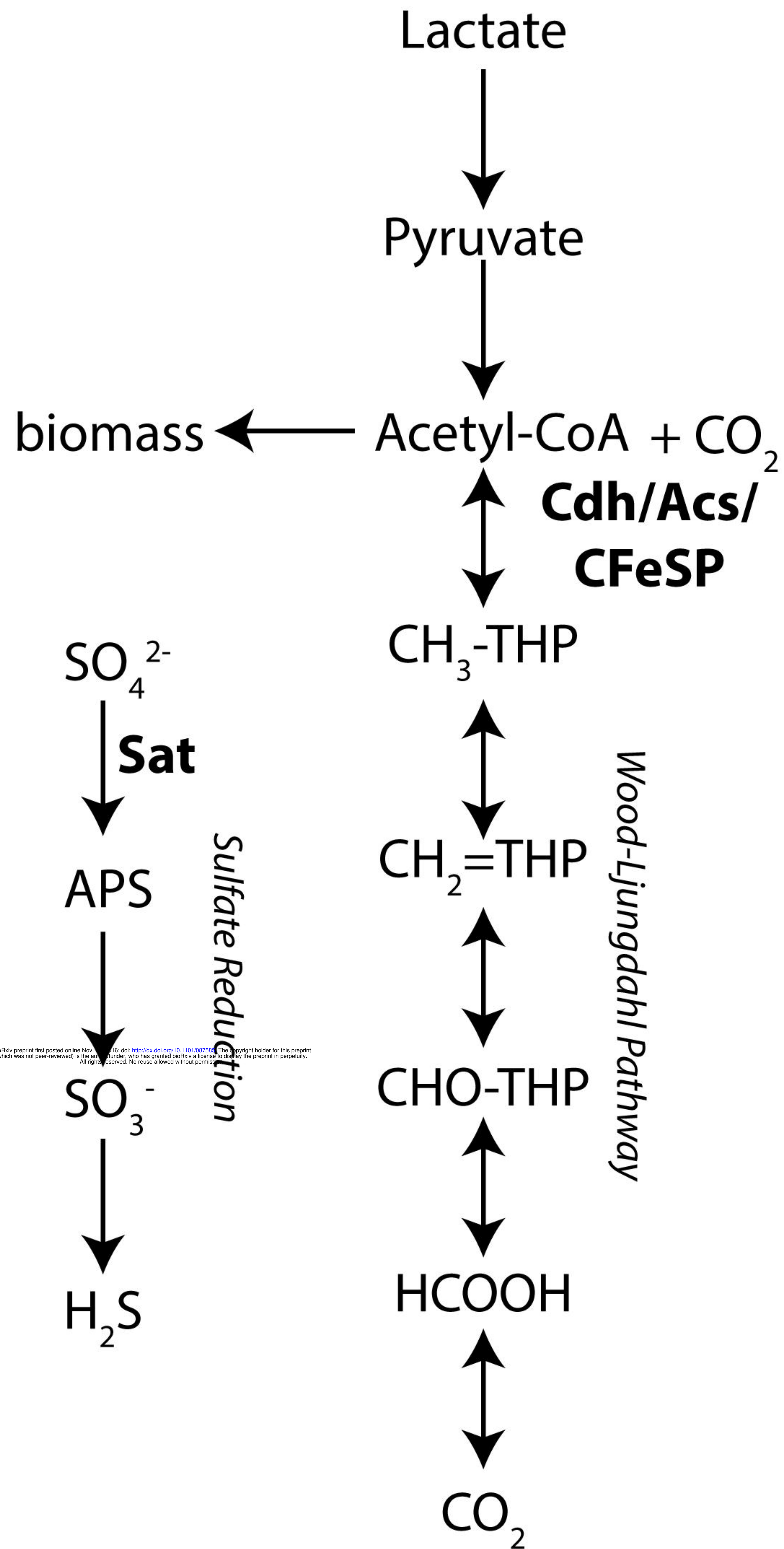


Figure 3

Desulfococcus multivorans



Methanosarcina acetivorans C2A

